Journal of Advances in Science and Technology
Vol. 18, Issue No. 1, March-2021, ISSN 2230-9659

Processing of Mechanical Properties Using High String Rate Test

Dr. Vishal Kumar*

Associate Professor, Department of Physics, Government Women PG College, Kandhla, District-Shamli, State-Uttar Pradesh

Abstract - Finite element analysis was used to examine the influence that polymer strings' mechanical qualities have on badminton racquets in this research. Experiments on commercially available polymer strings yielded the non-linear mechanical properties of the material. As a further consideration, we looked at how strain rate affects the mechanical properties of the polymer strings. It was first designed that the badminton racquet string plane numerical simulation algorithm. The mechanical properties of the polymer string were analyzed using a nonlinear elastic model (Yeoh model). The findings of the simulations were compared to those of the experiments. In this study, we examined the relationship between the mechanical properties of the polymer strings and the geometry of the badminton racquets.

Keywords - badminton; finite element analysis; string plane

----------X----------

INTRODUCTION

Musical instrument players must constantly retune their instruments due to the fact that the characteristics of their strings change substantially with time, temperature, and humidity. Tuning changes are common throughout a performance with nylon and natural gut strings. This may be done on instruments that have a fingerboard; on open stringed instruments, such as an open-stringed guitar, the musician must wait for a break in the song before correcting an out-of-tune instrument.

To compare the generated tone to the needed musical pitch, automated string tuning systems typically require the instrument to be switched into a certain tuning mode and the string to be plucked or hit. The string tension may then be adjusted with the help of a motor. In the event that the string is already significantly out of tune when the following note is played, even if this mechanism were converted for performance usage, it would be useless. When a string is not being played, a tuning system should make proactive modifications to preserve its pitch.

What's needed is some kind of method for determining a string's pitch, as well as predicting how temperature and humidity, as well as the passage of time, will affect it. String young's modulus must be taken into consideration when generating scaling factors for a particular tuning mistake, in order to ensure that the tuning control system is both stable and able to make necessary adjustments with the minimal number of repetitions. At its predicted operating point, the tensile "tangent modulus" (the stress/strain ratio for tiny perturbations) of the string is required.

The well-known equation gives a decent approximation to the fundamental frequency f1 of a stretched flexible string:

$$f_1 = \frac{1}{2L_V}\sqrt{\frac{F}{\mu}} = \frac{1}{2L_V}\sqrt{\frac{\sigma}{\rho}}$$

A cross-sectional area of A is equal to = F/A, where F is the tension of the string, and is its linear density. LV denotes its vibrating length, and denotes the density of the material. The tensile stiffness of the string and the amount it has been stretched define the string tension. Temperature and humidity may alter the string's young's modulus, as well as thermal expansion, which affects the string's tension. The initial tuning of the string and subsequent modifications, as well as variations in temperature and humidity, all have an effect on the linear density of the string.

Strings made of nylon have a relatively low young's modulus, but there is essentially no published information on how these strings respond to temperature and humidity variations. Stretched nylon strings act in a different manner from bulk nylon, as will be shown below. In this study, we focus on the effects of temperature fluctuation on nylon rather than humidity.

LITERATURE REVIEW

KUCHARSKA, MONIKA (2020) Presented here are experimental and theoretical findings from studies on the TRIP (Transformation Induced Plasticity) steel wire drawing method. Using two different

drawing speeds (1.6 and 6 m/s) and two different drawing schemes, the wiredrawing process was tested in both labs and in the field (low and high single reductions). High drawing speeds (6 m/s) resulted in greater mechanical property values for wires drawn with low single reduction than for wires drawn with high single reduction, according to the results. Drawing wires with a ferritic-pearlitic structure contradicts this phenomenon, which suggests it has to do with the TRIP structure and the existence of residual austenite that is turned into martensite during the deformation process. Finite element analysis using the Drawing 2D application was used to undertake a theoretical wire drawing process study to help shed light on this strange occurrence. As a result of the simulation, it was discovered that wires drawn at high drawing speeds with modest single reductions saw a significant rise in surface temperature, which might lead to the blockage of the transition of residual austenite into martensite and a consequent loss in Re. Further research will entail testing the quantity of austenite maintained in wires acquired during experimental tests in order to support this hypothesis.

CAMILO A F SALVADOR (2022) Mechanical characteristics and microstructures of 282 different multicomponent Ti-based alloys are summarized in this study. Chemical composition (in at. percent), phase components, young modulus, hardness, yield strength, ultimate strength, and elongation are all included in this datasheet. There is a comprehensive explanation of the processing steps and testing setup for each of the entries. Additional flags in the dataset indicate that high-resolution microstructural analysis was used, as well as the discovery of non-linear elastic responses during mechanical testing. When available, data on oxygen content and grain size are shown. Material scientists may use the specified qualities to tailor the data to their own requirements when it comes to the selection and development of new materials. Ingot metallurgy, followed by solubilization and water quench, is the most common method used to make -Ti alloys in the dataset (58 percent). In an open platform, the database is hosted and kept up-to-date. A few graphical representations of the dataset have been added for completeness.

REMIGIUSZ BŁONIARZ (2021) An investigation of the effects of thermomechanical processing (TMP) on micro alloyed steels under dynamic loading conditions was carried out by researchers. Dilatometric tests were used to select the deformation settings for the thermomechanical laboratory rolling procedures. We were able to create microstructures with varying compositions and morphologies of certain components while maintaining a consistent overall deformation value. It was decided to focus on samples that showed a particularly intricate and surprising portrayal of the resulting microstructures. Digital image correlation (DIC) and Split Hopkinson Pressure Bar (SHPB) dynamic loading were used to conduct blastomeric testing, which included compression and tensile tests, at strain rates of 1400 and 2000 s-1. Hardness and microstructural examination of samples deformed under these circumstances were carried out. A variety of TMP parameters may lead to the production of certain microstructures, which in turn lead to an appealing mechanical response under dynamic loading circumstances. Such popular structural materials as micro alloyed steels may now be used in novel ways.

WU, QIONG, MIAO, (2020) With their tiny size, surface effect, quantum tunneling effect, and prospective uses in conventional materials, medical devices, electrical devices, coatings, and other sectors, nanomaterials have received widespread attention. On the mechanical characteristics of nanomaterials, effects of nanoparticle size, fabrication technique, and grain boundary structures are discussed. Nanomaterials are discussed in terms of their current state of study and potential range of applications. Nano-materials are superior to regular materials because of their unique features. As a result, there will be more uses for nanomaterials in the future. Nanomaterials research is critical to the advancement of materials science.

NGUYEN, N.TC (2020) As a consequence of the extended processing durations required for mass manufacturing, the term "super plasticity" is used to characterize a material's capacity to survive massive plastic deformation in the form of a tensile elongation to more than 400 percent of its original length. Super plasticity at high strain rates of more than 102 s-1, which is necessary for practical industry-scale use, has often only been accomplished in aluminum and magnesium alloys with low tensile strength. High-pressure torsion of an Al9(CoCrFeMnNi)91 high-entropy alloy nanostructured at a strain rate of 5 102 s1 results in a superplastic elongation of 2000% of the original length. As a result of high-pressure torsion and restricted grain development during hot plastic deformation, high strain rate super plasticity may be achieved by grain boundary sliding accommodated by dislocation activity.

RESEARCH METHODOLOGY

Strings Tested

Nylon pedal harp strings from Bow brand and Pirastro were examined; eleven strings from the former and two from the latter. Table 1 displays the string diameters and bulk densities that were measured prior to testing in order to better understand their properties. For the string diameter measurements, many measurements were performed along the string and averaged in order to increase the measurement precision. Weighing known lengths of string allowed us to determine their mass and, thus, their initial density. Scales with a precision of 1 mg were used to weigh the majority of the strings, resulting in density estimations that were accurate to within one percent. The Pirastro strings, on the other hand, were weighed using a scale with a lesser precision, resulting in a 3 percent greater

density error range for string 13, one of the lightest strings examined.

Table 1. The set of nylon harp strings studied, showing the unstretched string parameters, the targetfundamental frequencies for testing and the plot styles used in the responses shown in the figures. The number in the first column provides a unique reference for each test string or string section. It can be used to cross-reference with the summary dataset submitted with this paper and the larger dataset available at https://doi.org/10.17863/CAM.9018. Strings 12 and 13 were from the Pirastro “Nycor Concert Harp” range. The other strings were all from the Bowbrand “Pedal Nylon” range. The nine test frequencies marked with an asterisk correspond to the expected operating points on the harp. These points are included in some of the figures as black circles.

No.	Note	Diameter (mm)	Bulk Density (kg/m^3)	Target Test Frequencies (Hz)	Plot Style	Comments
1	A4 (19)	1.193	1067	323	Red circle	Tested only at low humidity
6	A6 (5)	0.661	1089	429 *	Red circle (low hum.)	Tested at bothhumidity levels
2	A4 (19)	1.199	1068	323 *		
3	A4 (19)	1.194	1080	323 *		
10a	A2 (33)	2.362	1134	235 *		Higher density
13	A6 (5)	0.613	1074	429	Blue circle	
12	A4 (19)	1.280	1070	323	Blue circle	
8	A6 (5)	0.658	1097	174, 235, 287, 323, 375, 403, 429 *, 453	Black line	
14	A5 (12)	0.841	1072	174, 235, 287, 323, 375 *, 403, 429, 453	Red line	
5	A4 (19)	1.196	1076	174, 235, 287, 323 *, 375, 403	Blue line	
23a	A3 (26)	1.680	1151	174, 235, 287 *, 323, 360	Green line	Higher density
29	E3 (29)	1.894	1159	174, 235, 287, 323	Cyan line	Higher density
10b	A2 (33)	2.362	1134	174,235 *	Magenta line	Higher density

Many investigations relied on the usage of this collection of strings. An identifying number was issued to each string when it was originally weighed and measured. This number appears in the first column of Table 1. The string number was reinforced with a suffix letter if a string was lengthy enough to allow for numerous testing sections. Despite their apparent illogic, these initial identifying numbers have been kept in order to be consistent with results from other studies. There is a summary dataset accompanying this study, as well as a much larger thorough dataset, that uses these values. A piano scale is used to specify the note that each string in Table 1 is supposed to be played on. In brackets, you'll see the harp string number that corresponds to that note. Strings A3 and below had a much greater density than strings A4 and above; this shows that the two groups of string had different formulas or potentially different basic polymers.

The string plane was studied using a 3-dimensional Cartesian coordinate system. There were two definitions of plane and x1-direction: one for inside and one for outside. String plane surface (Figure 1) orthogonal directions X1 and X2 were designated as X1 and X2. Finite element analysis nodes were generated at all points where the main and cross threads met in advance of the computer simulation. Grommets were made with additional nodes and their displacements were restricted. The badminton strings were recreated using beam components placed between the nodes. Pictured here is how a cross string deforms, as seen in Figure 2. The strings before and after deformation are shown as dotted and solid lines, respectively. The main (vertical) and cross (horizontal) strings converge at these black circles. It is the distance between the kth and lth nodes, and it is the distance after deformation, which is L (,) Before deformation, horizontal and vertical string tensions are T and T, whereas post-deformation tensions are T (u) and T (u). u is the axial displacement of the strings. By changing the subscripts 1 to 2, you can see how the main text deforms in Figure 2. Based on a tennis racquet string-bed stiffness simulation algorithm, the

simulation code used in this investigation was formulated. During the development of the simulation code, string mechanical qualities and the nonlinearity of the geometrical shape of string planes were taken into account. Using the following equations, we determined the kth and lth nodes' forces in the x-direction:

$$f_3^{(k)} = \alpha\bar{T}(\bar{u})sin\theta = \alpha\frac{\bar{T}(\bar{u})}{\bar{L}^{(k,l)}}\left(u_3^{(k)} - u_3^{(l)}\right), f_3^{(l)} = -\alpha\bar{T}sin\theta = \alpha\frac{\bar{T}(\bar{u})}{\bar{L}^{(k,l)}}\left(u_3^{(l)} - u_3^{(k)}\right).$$

The node numbers are k and l in this example. u () is the kth node's displacement in the x-direction. is the angle formed by the pre- and post-deformation strings? The out-of-plane stiffness adjusting coefficient is. Because there were some strings that contributed to out-of-plane stiffness and others that didn't, we have the coefficient. The coefficient is taken to be 0.65 in this research.

The Coulomb friction model was used to simulate the in-plane stiffness of the string planes. If the in-plane force was larger than the maximum static friction force, the strings were considered to have slid. Tennis racquet string bed stiffness formula was used to compute the friction force. Equation (1) relates to T(u) for horizontal and vertical strings, respectively. The elongation of the strings increased the tension of the strings when the string plane was distorted. The axial elongation of the strings was used to compute the tension T (u) and T (u) of the strings. The deformation of the strings was represented using a different 3-dimensional Cartesian coordinate system (x′, x′, x′). All of the horizontal and vertical strings had their axial direction defined as x′, whereas the x′-direction was specified as the lateral direction. This equation was used to compute the axial (x′-direction) displacement of the strings u:

$$\bar{u} = \sqrt{(L^{(k,l)} + (u_1^{(k)} - u_1^{(l)}))^2 + (u_2^{(k)} - u_2^{(l)})^2 + (u_3^{(k)} - u_3^{(l)})^2} - L^{(k,l)}.$$

The following equation was used to compute the axial stretch of the strings:

$$\lambda = 1 + \frac{\bar{u}}{L^{(k,l)}}.$$

To mimic the strings' mechanical properties, an incompressible hyper elastic material was used. The Yeoh Model was used to apply the strain energy function W(C). This equation yielded the W(C) strain energy function:

$$W(\bar{C}) = C_{10}(\bar{I}_1 - 3) + \frac{C_{20}}{2}(\bar{I}_1 - 3)^2 + \frac{C_{30}}{3}(\bar{I}_1 - 3)^3.$$

A modified first invariant of a modified right Cauchy–Green tensor, C, is I's modified first invariant in this example. The partial differentiation of the strain energy function W(C) with regard to the right Cauchy–Green deformation tensor C yields the second Piola–Kirchhoff stress tensor S:

$$\boldsymbol{S} = 2\frac{\partial W(\bar{\boldsymbol{C}})}{\partial \boldsymbol{C}} + p\boldsymbol{C}^{-1}.$$

Hydrostatic pressure (p) may be determined using the boundary condition. The deformation gradient tensor F was used to transform the second Piola–Kirchhoff stress tensor S into the Cauchy stress tensor T. The following equation yields the Cauchy stress tensor T:

$$\boldsymbol{T} = \boldsymbol{FSF}^T = 2\frac{\partial W(\bar{\boldsymbol{C}})}{\partial \bar{I}_1}\begin{pmatrix} \lambda^2 - \frac{1}{\lambda} & 0 & 0 \\ 0 & 0 & 0 \\ 0 & 0 & 0 \end{pmatrix}.$$

For nonlinear mechanical properties, the string element T was determined as follows:

$$\bar{T} = T_{11}\mathrm{A} = 2\{C_{10} + C_{20}(\bar{I}_1 - 3) + C_{30}(\bar{I}_1 - 3)^2\}\left(\lambda^2 - \frac{1}{\lambda}\right)\mathrm{A}.$$

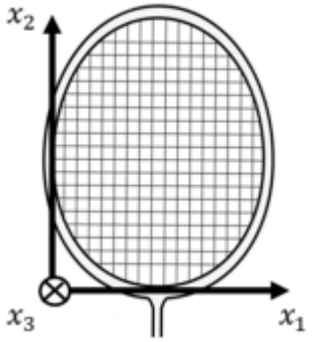

Figure 1: 3-Dimentional coordination system.

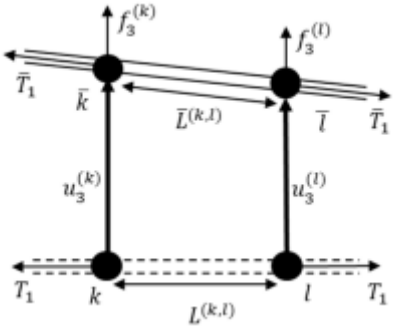

Figure 2: Deformation behavior of the string.

DATA ANALYSIS

Loading Test of Nylon Strings

Three specimens for the uniaxial tensile test were created for testing nylon threads. The string had a diameter of 0.7 mm and a length of 30 mm. Figure 3 depicts the specimens. It is indicated in Figure 4 that the uniaxial tensile tests were carried out on the strings utilizing a uniaxial loading machine (Autograph AG-20kNXplus). Figure 5 depicts the uniaxial tensile testing. The loading test used strain rates of 1.0 percent /s, 0.1 percent /s, and 0.01

percent /s. Figure 6 depicts the stress-strain correlations derived from uniaxial tensile testing. A link between stress and strain in nylon strings was not found to be affected by strain rate, as shown in Figure 6.

The following formula may be used to solve Equation (8):

$$\frac{T_{11}}{2(\lambda^2-\frac{1}{\lambda})} = C_{10} + C_{20}(\bar{I}_1 - 3) + C_{30}(\bar{I}_1 - 3)^2.$$

The relationships between $(\bar{I}_1 - 3)$ and $\frac{T_{11}}{2(\lambda^2-\frac{1}{\lambda})}$ Figure depicts the tensile loading test results.

the least squares approach as shown in Figure 7 as independent quantities.

Figure 3: One of the nylon specimens.

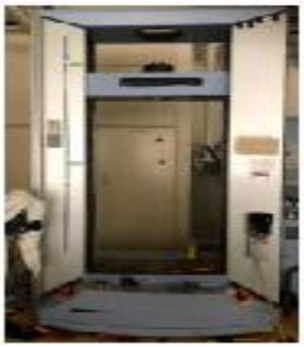

Figure 4: Uniaxial loading testing machine.

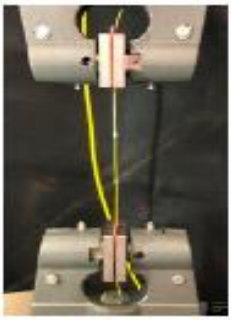

Figure 5: Uniaxial loading test.

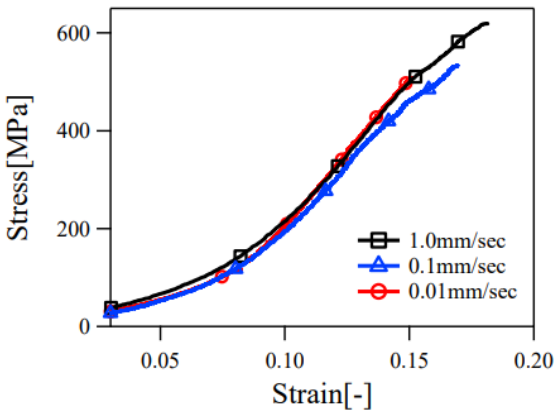

Figure 6: Stress-strain relationships of the nylon specimens.

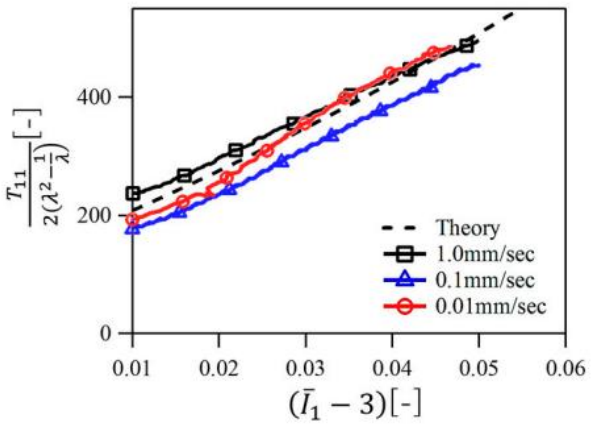

Figure 7: Relationship between

$(\bar{I}_1 - 3)$ and $\frac{T_{11}}{2(\lambda^2-\frac{1}{\lambda})}$.

Analysis of the String Plane Models of Three Badminton Racquets

For numerical simulation, three different badminton racquet string planes were created. Analysis models were added to the badminton racquet string planes (Racquet A, B, and C). Racquet A and Racquet B have almost identical string spacing. Racquet C's bottom string plane has more spacing between the strings than the higher string plane. Racquet A had the greatest string planes, whereas Racquet C had the smallest string planes. Figure 8 depicts the three racquets involved in this scenario. Polymer strings were used to apply line elements to the analysis models. In addition, the frames for the analysis models were the line components between the grommets. The string diameter was set at 0.7 mm and the starting tension at 106.76 N. The simulation algorithm was tweaked to use the nylon string material values listed in Section 3.1. The out-of-plane stiffness of the string planes was measured by applying a 10 N out-of-plane force to each node. Figure 9 depicts the end outcome. Racquet A's and Racquet B's string plane stiffness distributions decreased from the string plane edges toward the

center. Racquet C's bottom string plane had less stiffness than its higher string plane.

Figure 8: Three badminton racquets made by different companies, respectively

Effect of the Nonlinear Property of Polymer Strings

The out-of-plane stiffness of the string planes was numerically calculated using the analytical model of Racquet A's string planes in order to examine the impact of polymer strings' nonlinear properties. The analytical model's out-of-plane stiffness was estimated in two separate ways.

There were four nodes on the model in Figure 9a that received loads ranging from 10 N to 50 N for simulation scenario 1. Using the nonlinear characteristics of the polymer strings, the stiffness of badminton racquets' string planes was estimated. Hyperplastic model Equation (6) was used to describe the mechanical properties of the polymer strings in the nonlinear scenario. The nonlinear mechanical characteristics of the polymer strings were examined by comparing the computed results to the findings of the linear case. The constant tension of the strings in the linear example was 106.76 N. At an out-of-plane load of 50 N, the model's displacement is shown in Figure 10. Figure 11 depicts the load-displacement relationships at the analysis model's most deformed node. The polymer string's nonlinear mechanical properties were used to determine out-of-plane stiffness, which resulted in a higher value than the linear condition.

A 50 N out-of-plane load was applied to four adjacent nodes on the racquet depicted in Figure 9b for simulation scenario 2. Stiffness is illustrated in Figure 12 in relation to the location of x. The stiffness computed with and without the nonlinear effect is greater than the stiffness calculated without the nonlinear effect.

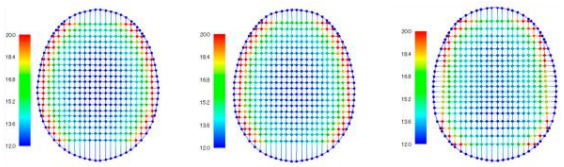

Figure 9: Out-of-plane stiffness of the string planes of the three racquets.

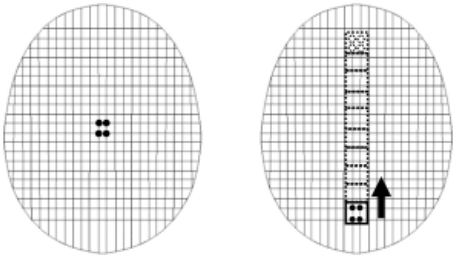

Figure 10: The positions applied to the load in the analysis model of the badminton racquet

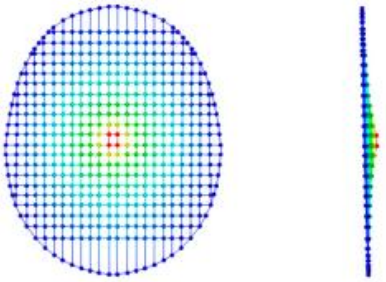

Figure 11: Deformations of the string plane when applying 50N to each node.

CONCLUSIONS

The out-of-plane stiffness of badminton racquet string planes was predicted using finite element analysis, which took into account the nonlinear mechanical properties of polymer strings. Nylon string uniaxial tensile testing provided the material properties used in the numerical simulation. In order to determine how the badminton racquet geometry and the polymer string mechanical properties affect the out-of-plane stiffness of the string planes, three different badminton racquets were tested. Using the simulation code provided in this article, badminton racquet string plane design optimization was possible.

REFERENCE

1. Kucharska, Monika &Wiewiorowska, Sylwia&Michalczyk, Jacek &Gontarz, Andrzej. (2020). The Influence of the Drawing Process on the Mechanical Properties of TRIP Steel Wires with 0.4% C Content. Materials. 13. 10.3390/ma13245769.
2. Salvador, Camilo & Lopes Maia, Eloá& da Costa, Fernando & Escobar, J.D. & Oliveira, J. P. (2022). A compilation of experimental data on the mechanical properties and microstructural features of Ti-alloys. Scientific Data. 9. 10.1038/s41597-022-01283-9.
3. RemigiuszBłoniarz (2021),” How the Thermomechanical Processing Can Modify

the High Strain Rate Mechanical Response of a Microalloyed Steel," Materials 2021, 14, 6062. https://doi.org/10.3390/ma14206062 https://www.mdpi.com/journal/materials
4. Wu, Qiong, Miao, Wei-shou, Zhang, Yi-du, Gao, Han-jun and Hui, David. "Mechanical properties of nanomaterials: A review" *Nanotechnology Reviews*, vol. 9, no. 1, 2020, pp. 259-273. https://doi.org/10.1515/ntrev-2020-0021
5. Nguyen, N.TC., Asghari-Rad, P., Sathiyamoorthi, P. *et al.* Ultrahigh high-strain-rate superplasticity in a nanostructured high-entropy alloy. *Nat Commun* **11,** 2736 (2020). https://doi.org/10.1038/s41467-020-16601-1
6. Kwan, M. Designing the World's Best Badminton Racket. Ph.D. Thesis, Aalborg University, Aalborg, Denmark, 2010.
7. Nasruddin, F.A.; Harun, M.N.; Syahrom, A.; Abdul Kadir, M.R.; Omar, A.H.; Oechsner, A. Finite Element Analysis on Badminton Racket Design Parameter, 1st ed.; Springer Informational Publishing: New York, NY, USA, 2016; pp. 27–32.
8. Allen, T.; Choppin, S.; Knudson, D. A Review of Tennis Racket Performance Parameters. Sports Eng. 2016, 19, 1–11
9. Blomstrand, E.; Demant, M. Simulation of a Badminton Racket. Master's Thesis, Chalmers University of Technology, Göteborg, Sweden, 2017.
10. Matsuda, A.; Nakui, M.; Hashiguti, T. Simulation of Mechanical Characteristics of Tennis Racket String Bed Considering String Pattern. Proceedings 2018, 2, 264.

Corresponding Author

Dr. Vishal Kumar*

Associate Professor, Department of Physics, Government Women PG College, Kandhla, District-Shamli, State- Uttar Pradesh